J Syst Sci Complex (2018) 31: 1510–1524

Chaos and Nonlinear Feedback Control of the Arch Micro-Electro-Mechanical System*

LUO Shaohua · LI Shaobo · TAJADDODIANFAR Farid

DOI: 10.1007/s11424-018-7234-5
Received: 9 July 2017 / Revised: 27 December 2017

Abstract This paper addresses a nonlinear feedback control problem for the chaotic arch micro-electro-mechanical system with unknown parameters, immeasurable states and partial state-constraint subjected to the distributed electrostatic actuation. To reflect inherent properties and design controller, the phase diagrams, bifurcation diagram and Poincare section are presented to investigate the nonlinear dynamics. The authors employ a symmetric barrier Lyapunov function to prevent violation of constraint when the arch micro-electro-mechanical system faces some limits. An RBF neural network system integrating with an update law is adopted to estimate unknown function with arbitrarily small error. To eliminate chaotic oscillation, a neuro-adaptive backstepping control scheme fused with an extended state tracking differentiator and an observer is constructed to lower requirements on measured states and precise system model. Besides, introducing an extended state tracking differentiator avoids repeated derivative for the virtual control signal associated with conventional backstepping. Finally, simulation results are presented to illustrate feasibility of the proposed scheme.

Keywords Arch micro-electro-mechanical system, chaos suppression, Neuro-adaptive backstepping, nonlinear feedback control, uncertainty.

1 Introduction

The micro-electro-mechanical system (MEMS) has received considerable attention in the domain of platform stabilization, activity monitoring, sport equipment, robotics, filters, etc.[1−5].

LUO Shaohua · LI Shaobo (Corresponding author)
Key Laboratory of Advanced Manufacturing Technology, Ministry of Education, Guizhou University, Guiyang 550025*, China; School of Mechanical Engineering, Guizhou University, Guiyang* 550025*, China.*
Email: hua66com@163.com; lishaobo@gzu.edu.cn.
TAJADDODIANFAR Farid
Department of Mechanical Engineering, Erik Jonsson School of Engineering and Computer Science, The University of Texas at Dallas, Richardson TX 75080*, USA*. Email: farid.tajaddodianfar@utdallas.edu.
*This research was supported by the National Natural Science Foundation of China under Grant Nos. 51505170, 51475097 and 51505045, Basic and Frontier Research Program of Chongqing Municipality under Grant Nos. cstc2016jcyjA0584 and cstc2016jcyjA0441), Project of Introduction of Talents of Guizhou University (No. [2017]27) and Key Scientific Research Program of Guizhou Province under Grant No. [2017]3001).
◇ *This paper was recommended for publication by Editor LIU Yungang.*

The works focusing on nonlinear dynamics of the arch micro-electro-mechanical system have been reported. The transient finite electro-elasto-dynamic deformations of the electrically conducting undamped clamped-clamped beam is studied[6]. The nonlinear dynamics of the arch micro-electro-mechanical system in the manner of experiment and theory is investigated and this system is recommended to use in band pass filters[7,8]. Chaotic oscillation of the arch micro-electro-mechanical system is studied with aid of analytical and numerical methods under the harmonic AC and static DC electrostatic actuation[9]. Chaos behaviors of the harmonically excited curved carbon nanotube are presented based on numerical simulations[10]. Researchers have spent much effort on realm of chaos. Then various methods have been reported to realize the chaos controlling. To get a critical value, a Melnikov function in a resonant gas sensor is employed under harmonic electrostatic load[11]. A chaos prediction scheme for the micro-electro-mechanical system with both symmetric and asymmetric double-well potential functions is developed[12]. A Melnikov method is introduced to distinguish chaotic phenomenon of the micro-electro-mechanical system and then a fuzzy control method with an adaptive law is proposed to suppress chaos[1].

The OGY method[13], linear and nonlinear feedback control[14,15], adaptive control[16] and time-delay feedback control[17] are considered as efficient tools for controlling chaotic vibration. However, these methods hardly achieve the goal of precision control when the micro-electro-mechanical system faces many uncertainties due to manufacturing defects and environmental variations. Sliding mode control (SMC) is an effective method to solve issues like time-varying properties, nonlinearities and bounded disturbances[18−20]. An SMC approach for a simulated microelectromechanical gyroscope system is proposed to measure angular velocity[21]. An adaptive SMC scheme of the micro-electro-mechanical gyroscope is presented to guarantee the system to track the given signal[22]. Unfortunately, its chattering phenomenon degrades the system performance. On this point, the terminal SMC is a finite-time control scheme as an improvement tool. A fast terminal SMC controller is designed to suppress chaos of the micro-electro-mechanical system with uncertainty and external disturbance[23]. But if we ignore issues such as inaccurate mathematical models and unmeasured variables limited by the micro-machined sensors, the nonlinear feedback control becomes meaningless.

For immeasurable states, the state observer is an effective resolution for the control system[24,25]. The Kalman filter as an optimal estimator is used to minimize the observation error in the presence of measurement noises and internal noises[26]. A parameterized state observer is developed for nonlinear dynamic systems with uncertain dead-zone nonlinearity[27]. An extended state observer which can cope with uncertainties, disturbances and sensor noises in nonlinear system is developed to achieve goal of active disturbance rejection control[28]. The arch micro-electro-mechanical system can suffer from state constraints such as physical stoppages, saturations and safety requirements in real conditions. This constraint violation leads to serious hazard for system stability. The existing solutions to deal with constraints are the model predictive control and barrier Lyapunov function[29]. The stabilization problem for a class of nonlinear strict-feedback systems with disturbances and time delays is solved[30]. However, this method leaves us with a problem, how to overcome “explosion of complexity”.

For this issue, many useful tools like fuzzy logic system, extended state observer, filter and neural network can be adopted to avoid repeated computation of derivative function[25,31,32].

Some achievements have been made, but some key issues have not been settled appropriately. Now the achievements mainly gather together in nonlinear dynamics and chaos prediction in this type of arch micro-electro-mechanical system. To the best knowledge of the authors, chaos and nonlinear feedback control of the arch micro-electro-mechanical system have not been investigated. We design a nonlinear feedback controller for the arch micro-electro-mechanical system which is characterised by fully unknown parameters, chaotic vibration, state constraint and unmeasured states. The indicators like phase diagrams, bifurcation diagram, Poincare section, etc. reveal that the arch micro-electro-mechanical system has chaotic characteristics. In the controller design, a state observer which lowers the requirements of physical sensors is employed to observe unmeasured system states, and a radial basis function (RBF) neural network which lifts restrictions on accurate models and parameters is introduced to achieve estimation of unknown function. An extended state tracking differentiator is used to deal with the "explosion of complexity" of traditional backstepping. By fusing observer, tracking differentiator and neural network into adaptive backstepping controller can realize nonlinear feedback control and suppress chaotic vibration. It is proved that the constraint is not transgressed with help of barrier Lyapunov function and all signals in the closed-loop system are bounded. Simulation results verify the effectiveness of our scheme.

2 System Modeling and Mathematical Preliminaries

The schematic diagram of the arch micro-electro-mechanical system is shown in Figure 1. Based on Euler-Bernoulli beam, the non-dimensionalized math equation of the arch micro-electro-mechanical system is expressed as[9,33]

$$\ddot{q}(t)+\mu\dot{q}(t)+\left(1+2h^2\alpha_1\right)q(t)-\frac{\beta\left(1+2R\cos\left(\omega_0 t\right)\right)}{2b_{11}\sqrt{\left(1+h-q(t)\right)^3}}-3\alpha_1 hq^2(t)+\alpha_1 q^3(t)+u(t)=0, \quad (1)$$

where μ, h, α_1, β, R, b_{11} are the dimensionless parameters, $q(t)$ denotes the state variable, ω_0 represents for the frequency and $u(t)$ is the control input.

Let $x_1=q(t)$, $x_2=\dot{q}(t)$ be new variables, then (1) is rewritten as

$$\begin{cases} \dot{x}_1=x_2, \quad y=x_1 \\ \dot{x}_2=-\mu x_2-\left(1+2h^2\alpha_1\right)x_1+\dfrac{\beta\left(1+2R\cos\left(\omega_0\tau\right)\right)}{2b_{11}\sqrt{\left(1+h-x_1\right)^3}}+3\alpha_1 hx_1^2-\alpha_1 x_1^3+u(t), \end{cases} \quad (2)$$

where the system output satisfies the constraint condition, that is, $|y|\le k_{c1}$, where $k_{c1}>0$.

The estimation value $\widehat{f}_{\mathrm{rbf}}(X)$ of unknown nonlinear item $f_{\mathrm{rbf}}(X)$ can be defined by RBF neural network such that[34]

$$\widehat{f}_{\mathrm{rbf}}(X,\theta(t))=\theta^{\mathrm{T}}(t)\,\xi(X), \quad (3)$$

where $\theta=[\theta_1,\theta_2,\cdots,\theta_l]^{\mathrm{T}}\in R^l$ denotes weight vector with node number $l>1$, $X\subset R^n$ denotes input vector, and $\xi(X)=[\xi_1(X),\xi_2(X),\cdots,\xi_l(X)]^{\mathrm{T}}\in R^l$ with $\xi_i(X)$ being Gaussian

functions which can be expressed as

$$\xi_i(X) = \exp\left[-\frac{(X-\mu_i)^{\mathrm{T}}(X-\mu_i)}{2\sigma_i^2}\right], \quad i = 1, 2, \cdots, l, \tag{4}$$

where σ_i means the width of Gaussian function, and $\mu_i = [\mu_{i1}, \mu_{i2}, \cdots, \mu_{in}]^{\mathrm{T}}$ denotes the center of receiving area.

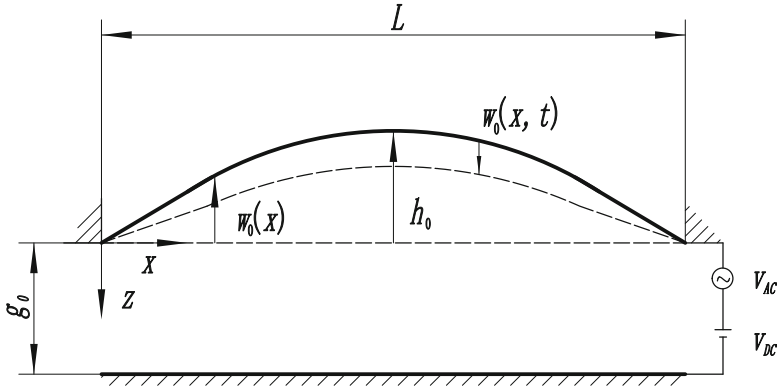

Figure 1 Schematic diagram of the arch micro-electro-mechanical system

We obtain a neural network in the form of (3) such that

$$\sup_{X \in D_X} \left| f_{\mathrm{rbf}}(X) - \theta^{\mathrm{T}}(t)\,\xi(X) \right| \leq \varepsilon, \tag{5}$$

where $\varepsilon > 0$, Ω_θ and D_X denote the compact set of suitable bounds of $\theta(t)$ and X, respectively. Let ideal parameter θ^* equal to

$$\arg\min_{\theta \in \Omega_\theta} \left[\sup_{X \in D_X} \left| f_{\mathrm{rbf}}(X) - \widehat{f}_{\mathrm{rbf}}(X, \theta) \right| \right].$$

$\widetilde{\theta}(t) = \theta(t) - \theta^*(t)$ exists.

Assumption 2.1 The reference trajectory x_r is bounded by $x_r \leq |x_u|$ and $\dot{x}_r$ is also bounded.

Lemma 2.1 (see [29]) *For $k_{b_i} > 0, i = 1, 2, \cdots, n$, define $Z := \{s \in \mathbb{R}^n : |s_i| < k_{b_i}, i = 1, 2, \cdots, n\} \subset \mathbb{R}^n$ and $N := \mathbb{R}^l \times Z \to \mathbb{R}^{l+n}$ as open sets.*

Consider the system

$$\dot{\eta} = h_e(t, \eta), \tag{6}$$

where $\eta := [w, s]^{\mathrm{T}} \in N$, and $h_e : \mathbb{R}_+ \times N \to \mathbb{R}^{l+n}$ is piecewise continuous in t and locally Lipschitz in Z. It has $U : \mathbb{R}^l \to \mathbb{R}_+$ and $V_i : s_i \to \mathbb{R}_+$ such that

$$V_i(s_i) \to \infty \ \text{ as } \ |s_i| \to k_{b_i}, \quad \mu_1(\|w\|) \leq U(w) \leq \mu_2(\|w\|), \tag{7}$$

where μ_1 and μ_2 are class K_∞ functions.

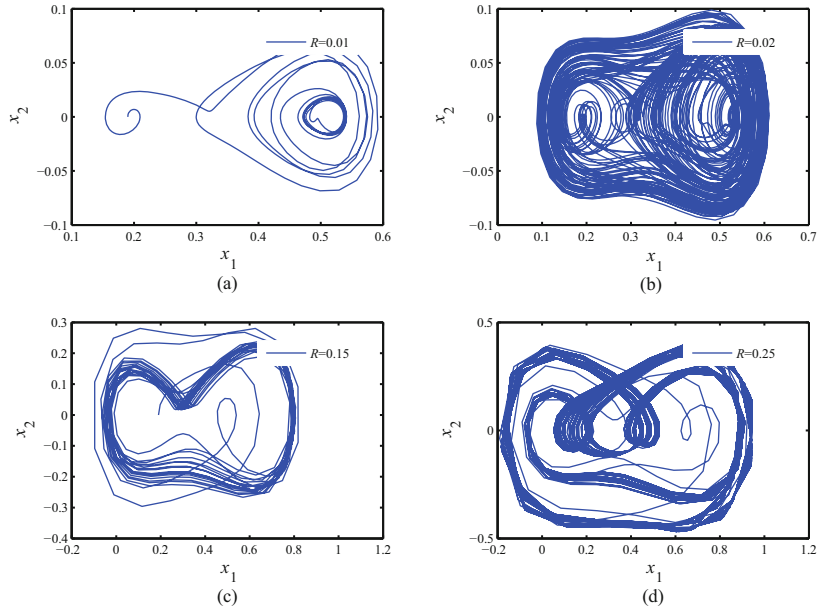

Figure 2 Phase diagrams for different R

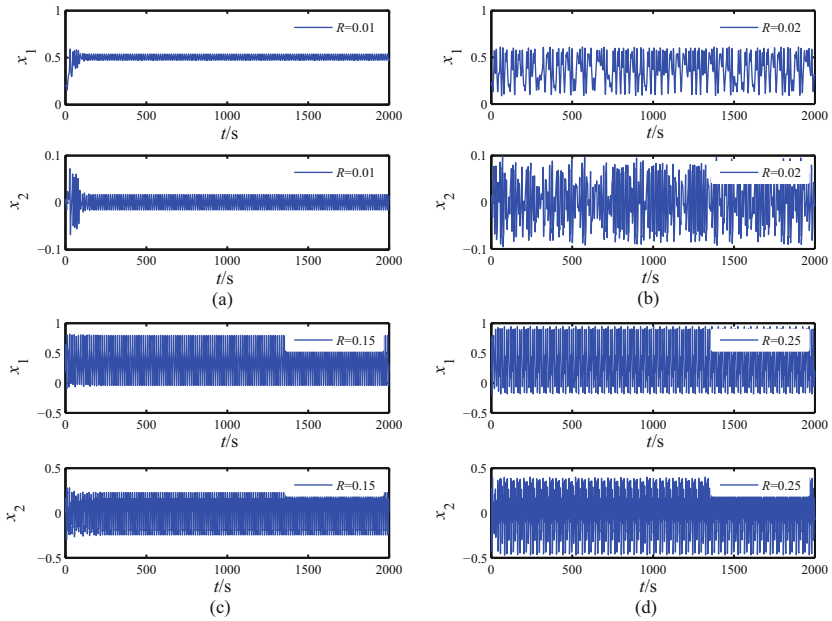

Figure 3 Time histories for different R

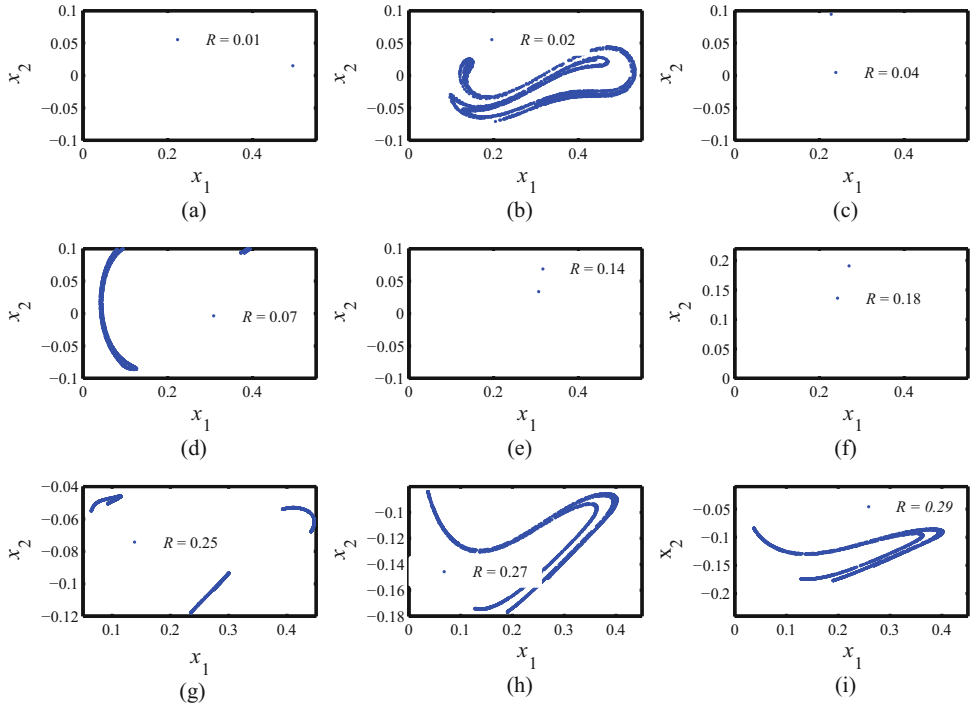

Figure 4 Poincare section for different R

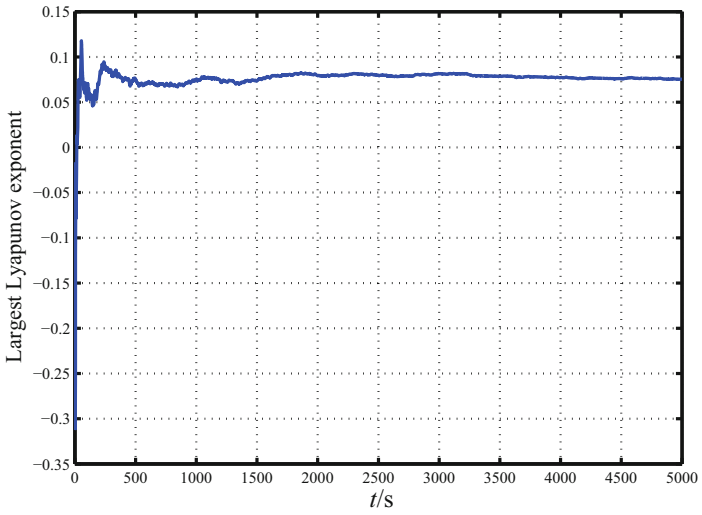

Figure 5 The largest Lyapunov exponent

Suppose that $V(\eta) := \sum_{i=1}^{n} V_i(s_i) + \mathrm{U}(w)$ and $s_i \in (-k_{b_i}, k_{b_i})$. If the inequality holds

$$\dot{V} = \frac{\partial V}{\partial \eta} h_e \leq 0, \tag{8}$$

then s_i remains in the set $s_i \in (-k_{b_i}, k_{b_i}), \forall t \in [0, \infty)$.

We study nonlinear dynamics of the arch micro-electro-mechanical system by setting parameters $\alpha_1 = 7.993$, $\beta = 119.9883$, $h = 0.3$, $R = 0.02$, $\mu = 0.1$, $\omega_0 = 0.4706$ and $u(t) = 0$. And we use the fourth-order Runge-Kutta algorithm to solve the differential equation system. Figures 2–3 show chaotic vibration of the arch micro-electro-mechanical system by using phase diagrams and time histories under different excitation amplitude R. The Poincare map exposes the route of chaotic vibration. In Figures 4(a), (c), (e) and (f), there exist the fixed points. In Figures 4(i) and (h), the attracting invariant orbit expands as R decreases. As R further decreases, the invariant orbit begins to distort from Figures 4(g) and (d). When R reaches to 0.02, the phase is unstable and chaos appears in Figure 4(b).

The Lyapunov exponent which is plotted in Figure 5 presents the positive value in a short time. It is obvious that the arch micro-electro-mechanical system involves "chaotic vibration". In Figure 6, the bifurcation diagram of the arch micro-electro-mechanical system which shows the state x_1 versus the excitation amplitude R is given to analyze periodic oscillation states and chaos motions. Then the dynamic behavior from regular motion and irregular motion is observed more completely.

Chaotic oscillation associated with the arch micro-electro-mechanical system inevitably leads to the deterioration of the system performance. So it becomes very important to provide an effective control scheme to suppress chaotic oscillation of the arch micro-electro-mechanical system.

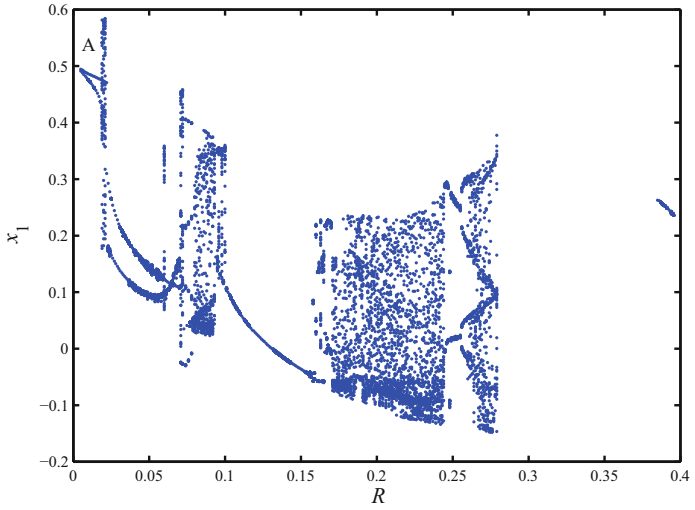

Figure 6 Bifurcation diagram

3 Nonlinear Feedback Controller Design

We use an extended state observer to estimate immeasurable variables as[28]

$$\begin{cases} \dot{\zeta}_0 = \varsigma_0, \quad \varsigma_0 = -k_0|\zeta_0 - f_r(t)|^{n/(n+1)}\text{sign}(\zeta_0 - f_r(t)) + \zeta_1, \\ \vdots \\ \dot{\zeta}_{n-1} = \varsigma_{n-1}, \quad \varsigma_{n-1} = -k_{n-1}|\zeta_{n-1} - \varsigma_{n-2}|^{0.5}\text{sign}(\zeta_{n-1} - \varsigma_{n-2}) + \zeta_n, \\ \dot{\zeta}_n = -k_n\text{sign}(\zeta_n - \varsigma_{n-1}), \end{cases} \tag{9}$$

where ζ_0 denotes the estimator of the given signal $f_r(t)$, $k_i > 0, i = 1, 2, \cdots, n$.

By using (9) to obtain the information of state variables, the extended state observer for the arch micro-electro-mechanical system can be written as

$$\begin{cases} \dot{\widehat{x}}_1 = \varsigma_0\dot{\widehat{x}}_1 = \varsigma_0, \quad \varsigma_0 = -k_0|\widehat{x}_1 - x_1|^{2/3}\,\text{sign}(\widehat{x}_1 - x_1) + \widehat{x}_2, \\ \dot{\widehat{x}}_2 = \varsigma_1 + u(t), \quad \varsigma_1 = -k_1|\widehat{x}_2 - \varsigma_0|^{0.5}\,\text{sign}(\widehat{x}_2 - \varsigma_0) + \widehat{x}_3, \\ \dot{\widehat{x}}_3 = -k_2\,\text{sign}(\widehat{x}_3 - \varsigma_1). \end{cases} \tag{10}$$

The finite-time convergence of (10) is guaranteed when the observing errors $\widetilde{x}_i = \widehat{x}_i - x_i, i = 1, 2, 3$ satisfy $|\widehat{x}_i - x_i| \le l$, where $\widehat{x}_i$, $i = 1, 2, 3$ are the estimation of $x_i, i = 1, 2, 3$, $l > 0$.

We adopt an extended state tracking differentiator to get a better evaluation of uncertain item as

$$\begin{cases} \dot{\varpi}_{j1} = \varpi_{j2} - \beta_{j1}\text{fal}(\delta_e, \eta_{ej}), \\ \dot{\varpi}_{j2} = -\beta_{j2}\text{fal}(\delta_e, \eta_{ej}) \end{cases} \tag{11}$$

with nonlinear function

$$\text{fal}(\delta_e, \eta_{ej}) = \begin{cases} \dfrac{\eta_{ej}}{\delta_e^{1-\alpha_e}}, & |\eta_{ej}| \le \delta_e, \\ |\eta_{ej}|^{\alpha_e}\text{sign}(\eta_{ej}), & |\eta_{ej}| > \delta_e, \end{cases}$$

where β_{ji}, $j = 1, 2, \cdots, n$, $i = 1, 2$ denote the feedback gain, η_{ej} is the tracking differentiator error, $\delta_e > 0$, $\alpha_e > 0$.

Define the first error function as $s_1 = x_1 - x_r$. Choose the symmetric barrier Lyapunov function candidate[29]

$$V_1 = \frac{1}{2}\ln\frac{k_{b_1}^2}{k_{b_1}^2 - s_1^2}, \tag{12}$$

where $k_{b_1} = k_{c_1} - x_u$ and the constraint $|s_1| < k_{b_1}$ is not violated.

Because the state variable x_2 is immeasurable, we employ an extended state observer to evaluate it. Define the second error function as $\widehat{s}_2 = \widehat{x}_2 - \alpha_2$, where α_2 denotes the virtual control.

The derivative of V_1 along the solutions of (2) is calculated as

$$\dot{V}_1 = \frac{s_1(\widehat{s}_2 + \alpha_2 - \dot{x}_r - \widetilde{x}_2)}{\kappa_1}, \tag{13}$$

where $\kappa_1 = k_{b_1}^2 - s_1^2$.

Then, the virtual control can be obtained as $\alpha_2 = -\kappa_1 c_1 s_1 + \dot{x}_r$, where $c_1 > 0$. It has

$$\dot{V}_1 \leq -c_1 s_1^2 + \frac{\widehat{s}_2 s_1}{\kappa_1} + l\left|\frac{s_1}{\kappa_1}\right|. \tag{14}$$

The derivative of $\widehat{s}_2$ is given as

$$\dot{\widehat{s}}_2 = f_{un}(\cdot) + u(t) + \dot{\widetilde{x}}_2 - \dot{\alpha}_2, \tag{15}$$

where $f_{un}(\cdot) = -\left(1 + 2h^2\alpha_1\right) x_1 + \frac{\beta(1+2R\cos(\omega_0 t))}{2b_{11}\sqrt{(1+h-x_1)^3}} - \mu x_2 - \alpha_1 x_1^3 + 3\alpha_1 h x_1^2$.

Note that $f_{un}(\cdot)$ has complicated nonlinear characteristics. The derivative of α_2 increases the design complexity and computation load, and the system parameters such as $\mu, h, \alpha_1, \beta, \omega_0, R$, b_{11} may be unknown or less precise because of impacts from manufacturing defects, external environmental variations, modeling error, etc. Meanwhile, Tajaddodianfar, et al.[9] revealed that the system parameters variations resulted in chaotic vibration. Given these, it is desperately searching for ways to overcome negative factors and nonlinear characteristics in controller design. We employ the RBF neural network to approximate nonlinear function such that $f_{un}(\cdot) = \theta_2^{\mathrm{T}}(t) \cdot \xi_2(x_1, \widehat{x}_2) + \varepsilon_2(x_1, \widehat{x}_2)$, where $\varepsilon_2(x_1, \widehat{x}_2) > 0$.

To reduce the computation burden, we take actions to decrease the number of weight vector for the RBF neural network. Using the Young's inequality, one has[35]

$$\theta_2^{\mathrm{T}}(t)\,\xi_2(x_1, \widehat{x}_2) = \frac{1}{2\nu_2^2}\psi_2(t)\,\xi_2^{\mathrm{T}}(x_1, \widehat{x}_2)\,\xi_2(x_1, \widehat{x}_2) + \frac{\nu_2^2}{2}, \tag{16}$$

where $\psi_2(t) = \left\|\theta_2^{\mathrm{T}}(t)\,\theta_2(t)\right\|$, $\nu_2 > 0$, $\widetilde{\psi}_2(t) = \widehat{\psi}_2(t) - \psi_2(t)$ holds, $\widehat{\psi}_2(t)$ is the estimation of $\psi_2(t)$.

Select the Lyapunov function candidate

$$V_2 = V_1 + \frac{1}{2}\widehat{s}_2^2 + \frac{1}{2\gamma_2}\widetilde{\psi}_2^2(t), \tag{17}$$

where $\gamma_2 > 0$.

Introducing an extended state tracking differentiator to evaluate $\dot{\alpha}_2$, the time derivative of V_2 can be written as

$$\dot{V}_2 = \dot{V}_1 + \widehat{s}_2\left(f_2(\cdot) + u(t) + \dot{\widetilde{x}}_2 - \varpi_{22}\right) + \frac{1}{\gamma_2}\widetilde{\psi}_2(t)\,\dot{\widehat{\psi}}_2(t). \tag{18}$$

From (11), we get $\eta_{e2} = \varpi_{21} - \alpha_2$. There exists an inequality as $|\varpi_{22} - \dot{\alpha}_2| \leq \eta_x$. According to (10), $\dot{\widetilde{x}}_2$ is obtained as

$$\dot{\widetilde{x}}_2 = -k_1|\widehat{x}_2 - \varsigma_0|^{0.5}\,\mathrm{sign}(\widehat{x}_2 - \varsigma_0) + \widetilde{x}_3. \tag{19}$$

Substituting(14) and (19) into (18) yields

$$\begin{aligned}\dot{V}_2 \leq\ & -c_1 s_1^2 + \widehat{s}_2\left(\frac{1}{2\nu_2^2}\psi_2(t)\,\xi_2^{\mathrm{T}}(x_1, \widehat{x}_2)\,\xi_2(x_1, \widehat{x}_2)\,\widehat{s}_2 + \frac{1}{2}\widehat{s}_2 + \overline{\varepsilon}_2 + u(t) - \varpi_{22} + \frac{s_1}{\kappa_1}\right) \\ & + \frac{1}{\gamma_2}\widetilde{\psi}_2(t)\,\dot{\widehat{\psi}}_2(t) + \frac{\nu_2^2}{2} + l\left|\frac{s_1}{\kappa_1}\right| + |\widehat{s}_2|\,l,\end{aligned} \tag{20}$$

where $|\varepsilon_2(x_1,\widehat{x}_2)|\leq\overline{\varepsilon}_2$.

Finally, the actual control with an update law is designed as

$$u(t)=-\left(c_{21}+\frac{1}{2}\right)\widehat{s}_2-\frac{s_1}{\kappa_1}-\frac{1}{2\nu_2^2}\widehat{\psi}_2(t)\,\xi_2^{\mathrm{T}}(x_1,\widehat{x}_2)\,\xi_2(x_1,\widehat{x}_2)\,\widehat{s}_2+\varpi_{22}-c_{22}\mathrm{sign}\widehat{s}_2, \quad (21)$$

$$\dot{\widehat{\psi}}_2(t)=\frac{\gamma_2}{2\nu_2^2}\xi_2^{\mathrm{T}}(x_1,\widehat{x}_2)\,\xi_2(x_1,\widehat{x}_2)\,\widehat{s}_2^2-m_2\widehat{\psi}_2(t), \quad (22)$$

where $c_{21}>0$, $c_{22}>0$, $m_2>0$.

Substituting (21) and (22) into (20) yields

$$\dot{V}_2\leq-c_1s_1^2-c_{21}\widehat{s}_2^2+\overline{\varepsilon}_2\widehat{s}_2-c_{22}|\widehat{s}_2|-\frac{m_2}{\gamma_2}\widetilde{\psi}_2(t)\,\widehat{\psi}_2(t)+\frac{\nu_2^2}{2}+l\left|\frac{s_1}{\kappa_1}\right|+|\widehat{s}_2|\,l. \quad (23)$$

Note $-\frac{m_2}{\gamma_2}\widehat{\psi}_2(t)\,\widetilde{\psi}_2(t)\leq-\frac{m_2}{2\gamma_2}\left|\widetilde{\psi}_2(t)\right|^2+\frac{m_2}{2\gamma_2}|\psi_2(t)|^2$. According to Lemma 2.1 and Young's inequality, (23) is simplified as

$$\dot{V}_2\leq(-c_1+0.5)\,s_1^2+(-c_{21}+0.5)\,\widehat{s}_2^2-\frac{m_2}{2\gamma_2}\left|\widetilde{\psi}_2(t)\right|^2+\frac{\nu_2^2}{2}+\frac{m_2}{2\gamma_2}|\psi_2(t)|^2+l^2. \quad (24)$$

Theorem 3.1 *Consider the arch micro-electro-mechanical system with unknown parameters, chaotic vibration, immeasurable states and partial state-constraint subjected to the distributed electrostatic actuation. If a third-order extended state observer is constructed as* (10)*, and the nonlinear feedback controller integrated with an update law* (22) *and an extended state tracking differentiator* (11) *is designed as* (21)*, then all signals of the closed-loop system are uniformly ultimately bounded and the output constraint is never violated.*

Proof Define the Lyapunov function as $V=\frac{1}{2}\ln\frac{k_{b_1}^2}{k_{b_1}^2-s_1^2}+\frac{1}{2}\widehat{s}_2^2+\frac{1}{2\gamma_2}\widehat{\psi}_2^2(t)$. Then, its derivative is derived as

$$\begin{aligned}\dot{V}&=\dot{V}_2\\&\leq-(c_1-0.5)\,s_1^2-(c_{21}-0.5)\,\widehat{s}_2^2-\frac{m_2}{2\gamma_2}\left|\widetilde{\psi}_2(t)\right|^2+\delta_0\\&\leq-\vartheta_0V+\delta_0,\end{aligned} \quad (25)$$

where $\vartheta_0=\min\{2\times(c_1-0.5),2\times(c_{21}-0.5),m_2\}$ and $\delta_0=\frac{\nu_2^2}{2}+\frac{m_2}{2\gamma_2}|\psi_2(t)|^2+l^2$.

Applying integral transformation for (25), one has

$$0\leq V(t)\leq\frac{\delta_0}{\vartheta_0}+\left(V(t_0)-\frac{\delta_0}{\vartheta_0}\right)\mathrm{e}^{-\delta_0(t-t_0)}\leq\frac{\delta_0}{\vartheta_0}+V(t_0). \quad (26)$$

Therefore, s_1, $\widehat{s}_2$ and $\widetilde{\psi}_2(t)$ are affiliated with a compact set

$$\Omega_x=\left\{\left(s_1,\widehat{s}_2,\widetilde{\psi}_2(t)\right)|V\leq V(t_0)+\frac{\delta_0}{\vartheta_0},\forall t\geq t_0\right\}. \quad (27)$$

From (26) it yields

$$\lim_{t\to\infty}s_1^2\leq\frac{2\delta_0}{\vartheta_0}. \quad (28)$$

Since $y(t)=s_1(t)+x_r$, $|s_1(t)|<k_{b_1}$ and $|x_r|\leq x_u$, it can be inferred that $|y(t)|<k_{b_1}+x_u=k_{c1}$. Hence, a conclusion can be drawn that the output y remains within the given constraint. Up to now, the proof of Theorem 3.1 is finished. ∎

4 Simulation

Following the instructions presented in Section 3, online-debugging is finished. The reference trajectory is selected as $x_r = 0.4\sin(2t)$ and the output constraint is subject to $|y| < k_{c1} = 0.43$. From the description above, we can see that $|s_1(t)| < k_{b_1} = 0.03$ holds. The parameters of the proposed controller are chosen as c_1= 8, c_{21} = 8, c_{22} = 0.1, γ_2 = 1, m_2 = 10, ν_2= 5. The parameters of the extended state observer are designed as k_0= 10, k_1= 10, k_2 = 10. The extended state tracking differentiator is adopted by appropriate selection of parameters as β_{21}=3, β_{22}=300, δ_e=0.022, α_e = 0.3. The initial value of $\widehat{\psi}_2(t)$ is 0.02. Moreover, the RBF neural network includes 9 nodes with the centers $\mu_i \in [-6, 6]$ and the width σ_i=3.

Figures 7(a)–(c) exhibit the results of the first error function for various R. It is obvious that tracking performance between the reference trajectory and actual trajectory is achieved. Figures 7(d)–(f) show that the tracking errors are less than ±0.03. $|y| < k_{c1}$ is guaranteed when the symmetric barrier Lyapunov function is introduced. Furthermore, comparing with phase diagrams presented in Figure 2 and time histories shown in Figure 3, the arch micro-electro-mechanical system immediately attains a steady state and its chaotic vibration subjected to the distributed electrostatic actuation is completely suppressed.

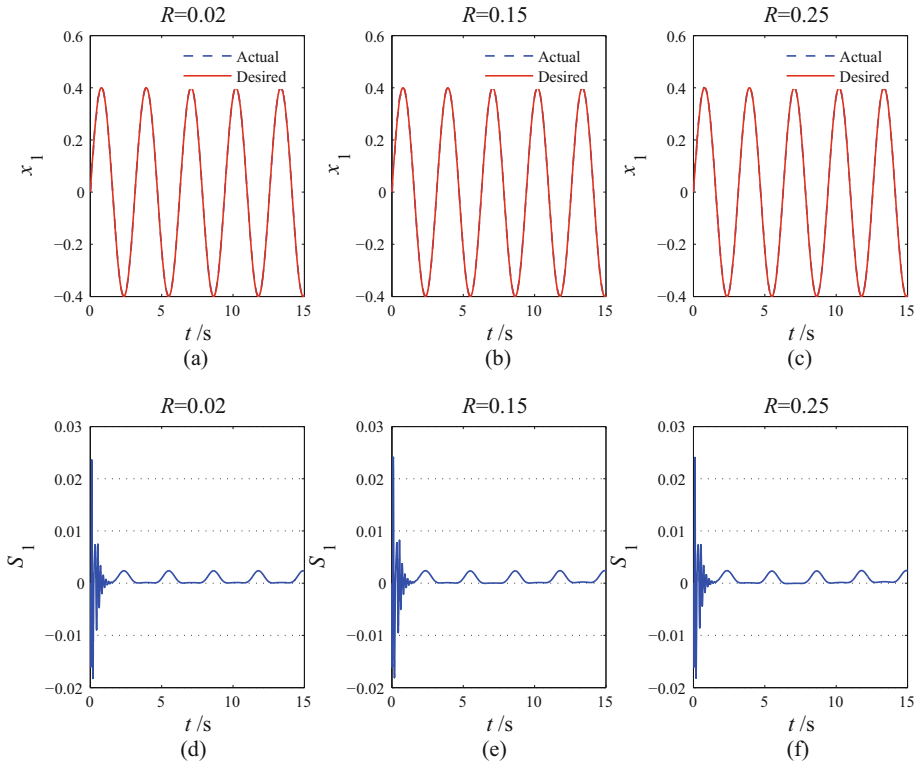

Figure 7 Tracking performance for different R

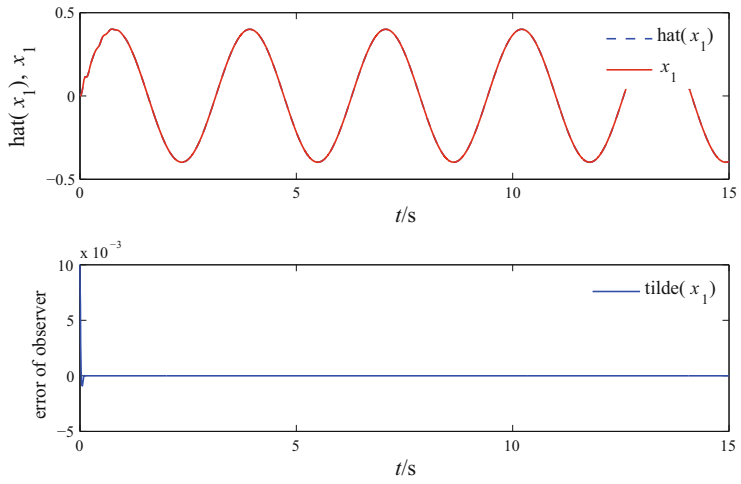

Figure 8 Observer performance between x_1 and $\widehat{x}_1$

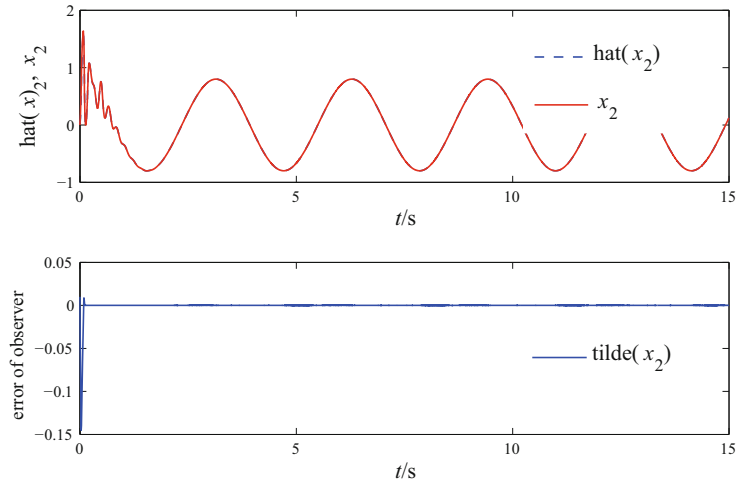

Figure 9 Observer performance between x_2 and $\widehat{x}_2$

Figures 8–9 reveal performance of the extended state observer for $x_i, i = 1, 2$. It can be seen that the extended state observer precisely evaluates actual signal, and then lifts the restrictions about sensors. Although the arch micro-electro-mechanical system has the characteristics of fully unknown parameters, partial state-constraint and chaotic vibration, observer errors converge to zero quickly with less oscillation.

Figure 10 depicts the control input of the arch micro-electro-mechanical system loaded by static DC voltage and harmonic AC actuation for various R. It can be seen that four curves of the arch micro-electro-mechanical system can remain consistent at a fast rate. It illustrates that the proposed controller has better anti-disturbance ability.

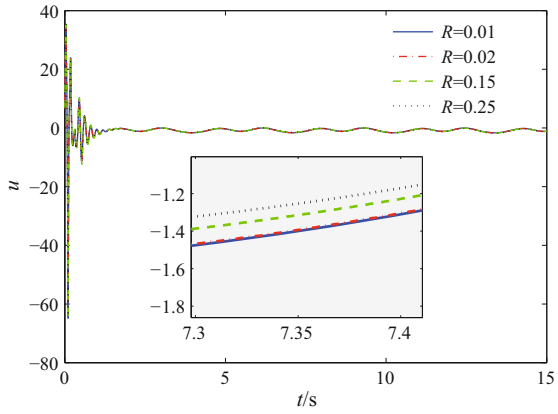

Figure 10 Control input for different R

5 Conclusion

The nonlinear feedback control scheme for the arch micro-electro-mechanical system which has features including fully unknown parameters, chaotic vibration, partial state-constraint and immeasurable states is the core of the present research based on the symmetric barrier Lyapunov function. The useful tools like phase diagrams, bifurcation diagram, Poincare section, etc. reveal that the arch micro-electro-mechanical system has the characteristics of chaotic oscillation. In the nonlinear feedback control, an extended state observer is employed to observe immeasurable variables and an RBF neural network system is introduced to evaluate unknown function with tiny error. The extended state tracking differentiator solves the "explosion of complexity" of the conventional backstepping. Then, by incorporating an observer, a tracking differentiator and an RBF neural network system into a neuro-adaptive backstepping controller can make system state to approximate the given signal precisely and suppress chaotic vibration. It is proved that the asymptotic tracking is achieved without constraint transgression, and that the closed-loop signals keep bounded. Finally, the performance of our scheme is demonstrated by simulation results.

References

[1] Haghighi H S and Markazi A H D, Chaos prediction and control in MEMS resonators, *Communications in Nonlinear Science and Numerical Simulation*, 2010, **15**(10): 3091–3099.

[2] Ghanbari A and Moghanni-Bavil-Olyaei M, Adaptive fuzzy terminal sliding-mode control of MEMS z-axis gyroscope with extended Kalman filter observer, *Systems Science and Control Engineering*, 2014, **2**(1): 183–191.

[3] Perez-Molina M and Prez-Polo MF, Fold-Hopf bifurcation, steady state, self-oscillating and

chaotic behavior in an electromechanical transducer with nonlinear control, *Communications in Nonlinear Science and Numerical Simulation*, 2012, **17**(12): 5172–5188.

[4] Luo S, Sun Q, and Cheng W, Chaos control of the micro-electro-mechanical resonator by using adaptive dynamic surface technology with extended state observer, *AIP Advances*, 2016, **6**(4): 045104.

[5] Zeng X and Jiang H, Liquid Tunable Microlenses based on MEMS techniques, *Journal of Physics D*, 2013, **46**(32): 474–480.

[6] Das K and Batra R, Pull-in and snap-through instabilities in transient deformations of microelectromechanical systems, *Journal of Micromechanics and Microengineering*, 2009, **19**(3): 035008.

[7] Younis M I, Ouakad H M, Alsaleem F M, et al., Nonlinear dynamics of MEMS arches under harmonic electrostatic actuation, *Journal of Microelectromechanical Systems*, 2010, **19**(3): 647–656.

[8] Tajaddodianfar F, Yazdi M R H, Pishkenari H N, et al., Classification of the nonlinear dynamics in an initially curved bistable micro/nano-electro-mechanical system resonator, *Micro and Nano Letters*, 2015, **10**(10): 583–588.

[9] Tajaddodianfar F, Pishkenari H N, and Yazdi M R H, Prediction of chaos in electrostatically actuated arch micro-nano resonators: Analytical approach, *Communications in Nonlinear Science and Numerical Simulation*, 2016, **30**(1): 182–195.

[10] Mayoof F N and Hawwa M A, Chaotic behavior of a curved carbon nanotube under harmonic excitation, *Chaos, Solitons and Fractals*, 2009, **42**(3): 1860–1867.

[11] Nayfeh A, Ouakad H, Najar F, et al., Nonlinear dynamics of a resonant gas sensor, *Nonlinear Dynamics*, 2010, **59**(4): 607–618.

[12] Miandoab E M, Pishkenari H N, Yousefi-Koma A, et al., Chaos prediction in MEMS-NEMS resonators, *International Journal of Engineering Science*, 2014, **82**(3): 74–83.

[13] Alasty A and Salarieh H, Controlling the chaos using fuzzy estimation of OGY and Pyragas controllers, *Chaos, Solitons and Fractals*, 2005, **26**(2): 379–392.

[14] Ho M C, Hung Y C, and Jiang I M, Synchronization between two chaotic systems with different order by using active control, *International Journal of Nonlinear Sciences and Numerical Simulation*, 2005, **6**(3): 249–254.

[15] Yassen M, Controlling chaos and synchronization for new chaotic system using linear feedback control, *Chaos, Solitons and Fractals*, 2005, **26**(3): 913–920.

[16] Shang F, Liu Y, and Zhang C, Adaptive practical tracking control by output feedback for a class of nonlinear systems, *Journal of Systems Science and Complexity*, 2010, **23**(6): 1210–1220.

[17] Sun Z, Xu W, Yang X, et al., Inducing or suppressing chaos in a double-well Duffing oscillator by time delay feedback, *Chaos, Solitons and Fractals*, 2006, **27**(3): 705–714.

[18] Roopaei M, Jahromi M Z, and Jafari S, Adaptive gain fuzzy sliding mode control for the synchronization of nonlinear chaotic gyros, *Chaos*, 2009, **19**(1): 377–411.

[19] Yang G, Kao Y, and Li W, Sliding mode control for Markovian switching singular systems with time-varying delays and nonlinear perturbations, *Discrete Dynamics in Nature and Society*, 2013, **2013**: 77–80.

[20] Liu L, Fu Z, and Song X, An adaptive sliding mode control of delta operator systems with input nonlinearity containing unknown slope parameters, *Journal of Systems Science and Complexity*, 2016, **30**(3): 1–15.

[21] Batur C, Sreeramreddy T, and Khasawneh Q, Sliding mode control of a simulated MEMS gyro-

scope, *ISA Transactions*, 2006, **45**(1): 99—108.

[22] Fei J and Batur C, A novel adaptive sliding mode control with application to MEMS gyroscope, *ISA Transactions*, 2009, **48**(1): 73–78.

[23] Zhankui S and Sun K, Nonlinear and chaos control of a micro-electro-mechanical system by using second-order fast terminal sliding mode control, *Communications in Nonlinear Science and Numerical Simulation*, 2013, **18**(9): 2540–2548.

[24] Li Y, Tong S, and Li T, Adaptive fuzzy backstepping control of static VAR compensator based on state observer, *Nonlinear Dynamics*, 2013, **73**(1–2): 133–142.

[25] Chen Q, Tao L, and Nan Y, Full-order sliding mode control for high-order nonlinear system based on extended state observer, *Journal of Systems Science and Complexity*, 2016, **29**(4): 978–990.

[26] Reif K and Unbehauen R, The extended Kalman filter as an exponential observer for nonlinear systems, *IEEE Transactions on Automatic Control*, 1999, **47**(8): 2324–2328.

[27] Zhou J, Wen C, and Zhang Y, Adaptive output control of nonlinear systems with uncertain dead-zone nonlinearity, *IEEE Transactions on Automatic Control*, 2006, **51**(3): 504–511.

[28] Sun G, Ren X, and Li D, Neural active disturbance rejection output control of multimotor servomechanism, *IEEE Transactions on Control Systems Technology*, 2015, **23**(2): 746–753.

[29] Tee K P, Ge S S, and Tay E H, Barrier Lyapunov functions for the control of output-constrained nonlinear systems, *Automatica*, 2009, **45**(4): 918–927.

[30] Wu J, Chen W, Yang F, et al., Global adaptive neural control for strict-feedback time-delay systems with predefined output accuracy, *Information Sciences*, 2015, **301**(C): 27–43.

[31] Yau H T, Wang C C, Hsieh C T, et al., Nonlinear analysis and control of the uncertain micro-electro-mechanical system by using a fuzzy sliding mode control design, *Computers and Mathematics with Applications*, 2011, **61**(8): 1912–1916.

[32] Chen Q, Tang X, Nan Y, et al., Finite-time neural funnel control for motor servo systems with unknown input constraint, *Journal of Systems Science and Complexity*, 2017, **30**(3): 579–594.

[33] Tajaddodianfar F, Pishkenari H N, Yazdi M R H, et al., Size-dependent bistability of an electrostatically actuated arch NEMS based on strain gradient theory, *Journal of Physics D*, 2015, **48**(24): 245503.

[34] Li Y, Lü H, and Jiao D, Prescribed performance synchronization controller design of fractional-order chaotic systems: An adaptive neural network control approach, *AIP Advances*, 2017, **7**(3): 035106.

[35] Luo S and Song Y, Chaos analysis-based adaptive backstepping control of the microelectromechanical resonators with constrained output and uncertain time delay, *IEEE Transactions on Industrial Electronics*, 2016, **63**(10): 6217–6225.